

# Track-Seeking Control using Input-Shaping Method to Reduce Vibration in HDD

Wimonrat Runghimmawan<sup>1)</sup>

Department of Data Storage Technology International,  
Faculty of Engineering,  
King Mongkut's Institute of Technology Ladkrabang,  
Bangkok 10502, Thailand  
(E-mail: wimonrat.runghimmawan@seagate.com<sup>1)</sup>)

Asst.Prof.Dr.Withit Chatlatanagulchai<sup>2)</sup>

Department of Mechanical Engineering,  
Faculty of Engineering,  
Kasetsart University,  
Bangkok 10900, Thailand  
(E-mail: fengwtc@ku.ac.th<sup>2)</sup>)

Assoc.Prof.Dr.Pitikhate Sooraksa<sup>3)</sup>

Department of Computer Engineering,  
Faculty of Engineering,  
King Mongkut's Institute of Technology Ladkrabang,  
Bangkok 10502, Thailand  
(E-mail: kspitikh@kmitl.ac.th<sup>3)</sup>)

**Abstract**— Hard disk drives are used for storage information in its recording disk or media. Actuator arm is mechanical part to move heads that fly over a track from any position to the target track. Accuracy signal and access time are the key parameters to control the actuator seeking position. However, the accuracy signal and access time are adverse when actuator moves faster and then the system create the residual vibration at the target track. The causes of the vibration are part from the fact that the reference signals, which are acceleration, velocity, and position, have high power spectrum energy over wide frequency range including over the actuator's natural frequency. The input shaping is convolved two signals at referent position signal and properly designed impulse signal. The impulse sequence produces an input signal to cancel residual vibration, then the result is smoother and the residual vibration is canceled in actuator-arm movement. Hence the residual vibration should be reduced by the recommended input shaping.

**Keywords**—Hard disk drive; Track seeking; Vibration; Input shaping;

## I. INTRODUCTION

Nowadays, hard disk drives use a combination of classical control, such as, PID compensators including notch filters to reduce the effects of high-frequency resonant modes. The actuator arm is mechanical part for moving head that fly over a track from any position to target track. The servo system of a hard disk drive is divided into three categories: 1) the track seeking, 2) the track settling, and 3) the track following stage. Figure 1 shows the Head Stack Assembly (HSA) and VCM Magnet in Hard disk drives. The gimbals and the suspensions help the heads for maintaining the constant flying height on an air bearing over the disks rotation. The heads fly over the disk surface is positioned by an actuator, which controls the movement of HSA is called servo system control. Voice coil motor (VCM) is widely used as the actuator in hard disk drives. VCM controls HSA and a selected head to follow a track (track

following stage) or to switch from one track to another (track seeking). The servo system is consisted of two main points: 1) the spindle motor servo system and 2) the actuator servo system; there are real-time embedded systems. The disks rotate at a constant speed and the actuator moves over the disk surface. This research scope to seeking mode that have 2 majors on design. Firstly mode switching condition is used for changing from seeking mode to the following mode that also required to smooth and minimize the residual vibration. Secondary velocity profiles require to be fast and robustness. The vibrations may exacerbate the head settling, make the effective seek time longer, and cause to acoustic problems. A settling mode is often used to smooth the transition.

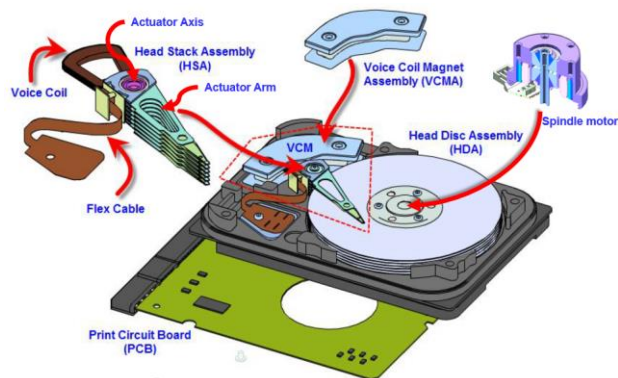


Figure 1: Head Stack Assembly (HSA) and VCM Magnet in HDA.

The motivation in this project interests in the track seeking on servo control are challenged to design for reducing vibration when the head move any track to target track. The design a servo controller that has the following physical constraints and design specification: 1) the control input does not exceed  $\pm 3$  Volts owing to physical constraints on the actual VCM actuator. 2) The overshoot and undershoot of track seeking are kept to less than  $0.5 \mu\text{m}$ , the limit of our measurement device for large

displacement. 3) The gain margin and phase margin of the overall design are, respectively, greater than 6 dB and 30°.

In active controls have proliferated, passive controls, especially those that use reference input shaping, are less well-known. Meckl and Seering (1988) reconstructed a bang-bang reference acceleration signal using ramped sine or versine basis functions. A cost function is penalized, weighing over removing the spectrum energy around the natural frequencies and approaching the bang-bang shape. Chatlatanagulchai et al. (2006) applied input shaping method with a two-link flexible-joint robot. Another shaping method was devised by Singer and Seering (1990.) Instead of shaping the reference acceleration, this method shapes the reference position directly by convoluting it with a properly designed impulse sequence. In theory, this impulse sequence is designed such that all impulse responses cancel each other producing vibration-free movement. Since the convolution with an impulse can be conveniently performed in real time, this method has received more attentions than the formal method, even though its appearance is still rare [2]. This paper applies the input shaping method to hard disk drives track seeking system. This servo system is made to follow any arbitrary angular position. It can be viewed as a model of actuator arm seeking movement only. A simple PID controller is used in the closed-loop system. The result is that the actuator arm can move with significantly less vibration when the shaped reference position is applied instead of an unshaped square-wave reference position.

## II. INPUT SHAPING BASIC

### A. Impulse Responses Cancellation

For a one-degree-of-freedom unforced linear system with damping, the response to an impulse with magnitude  $\hat{F}_1$  is given by

$$y(t) = \frac{\hat{F}_1 e^{-\zeta \omega_n (t-t_1)}}{m \omega_n \sqrt{1-\zeta^2}} \sin \sqrt{1-\zeta^2} \omega_n (t-t_1), \quad (1)$$

Where  $y$  is the response,  $\zeta$  is damping ratio,  $\omega_n$  is natural frequency,  $m$  is mass, and  $t_1$  is the time the impulse applies.

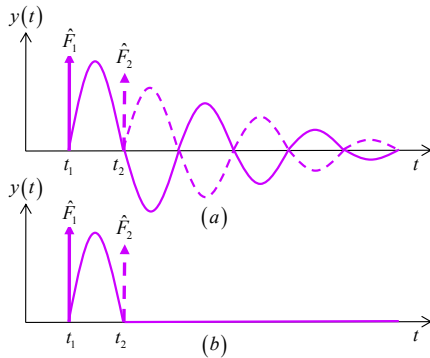


Figure 2: System response of two impulses [2].

The response  $y(t)$  above can be plotted as a solid line in Figure 2(a). Suppose there is another impulse  $\hat{F}_2$  applied at time  $t_2$ . when magnitude and timing are designed properly, its response (the dash line in Figure 2(a)) would be cancel with that of the first impulse producing vibration-free response Figure 2(b). Instead of  $N$  impulse, it can solve by trigon equation and shown that the amplitude of the sum of  $N$  impulse responses is given by

$$A = \sqrt{\left( \sum_{i=1}^N A_i \cos \beta_i \right)^2 + \left( \sum_{i=1}^N A_i \sin \beta_i \right)^2} \quad (2)$$

with  $A_i = \hat{F}_i e^{-\zeta \omega_n (t-t_i)} / (m \omega_n \sqrt{1-\zeta^2})$  and  $\beta_i = \sqrt{1-\zeta^2} \omega_n t_i$ .

Since the system want to have zero vibration, setting (2) to zero and  $t$  to  $t_N$  results in two constraints

$$\sum_{i=1}^N \hat{F}_i e^{-\zeta \omega_n (t_N-t_i)} \cos \sqrt{1-\zeta^2} \omega_n t_i = 0 \quad (3)$$

$$\text{and } \sum_{i=1}^N \hat{F}_i e^{-\zeta \omega_n (t_N-t_i)} \sin \sqrt{1-\zeta^2} \omega_n t_i = 0. \quad (4)$$

For two impulses, of which the first one applies at  $t_1 = 0$  and its impulse magnitude normalizes to  $\hat{F}_1 = 1$ ,  $\hat{F}_2$  and  $t_2$  can be found from the two equations above.

$$\hat{F}_2 = e^{-\frac{\zeta \pi}{\sqrt{1-\zeta^2}}} \text{ and } t_2 = \frac{\pi}{\omega_n \sqrt{1-\zeta^2}}.$$

### B. Robustness to Uncertainties in Natural Frequency and Damping Ratio

Since the amount of residual vibration left depends on the accuracy of the natural frequency ( $\omega_n$ ) and the damping ratio ( $\zeta$ ) used to compute  $\hat{F}_2$  and  $t_2$ , to increase the robustness of the input under variations of the natural frequency, we can set the derivatives, with respect to  $\omega_n$ , of (2) and (3) to zeros to obtain two more constraints

$$\sum_{i=1}^N \hat{F}_i t_i e^{-\zeta \omega_n (t_N-t_i)} \cos(\sqrt{1-\zeta^2} \omega_n t_i) = 0 \quad (4)$$

$$\text{and } \sum_{i=1}^N \hat{F}_i t_i e^{-\zeta \omega_n (t_N-t_i)} \sin(\sqrt{1-\zeta^2} \omega_n t_i) = 0. \quad (5)$$

The constraints (4) and (5) are reduced the sensitivity of the constraints (2) and (3) to change in  $\omega_n$  and can be used to solve for two additional unknowns  $t_3$  and  $\hat{F}_3$  of the third impulse. It can be shown that these constraints also apply to the robustness of the input under variations of the damping ratio. Letting  $t_1 = 0$  and  $\hat{F}_1 = 1$ , we can compute  $t_2$ ,  $\hat{F}_2$ ,  $t_3$ , and  $\hat{F}_3$  from (2)-(5) to be

$$t_2 = \frac{\pi}{\omega_n \sqrt{1-\zeta^2}}, \hat{F}_2 = 2e^{-\frac{\zeta\pi}{\sqrt{1-\zeta^2}}}, t_3 = \frac{2\pi}{\omega_n \sqrt{1-\zeta^2}}, \text{ and } \hat{F}_3 = e^{-\frac{2\zeta\pi}{\sqrt{1-\zeta^2}}}. \quad (6)$$

Increasing the robustness of the input shaping under variations of the damping ratio requires setting derivatives of (2) and (3) with respect to zeros. It turns out that this produces the same constraints as (4) and (5). To obtain even more robustness, we can continue to differentiate (4) and (5) to produce a new set of constraints for the fourth impulse and so on. However, more impulse so result could be robustness but in slower trajectory when implementing in the closed-loop system.

### III. INPUT SHAPING OF A HARD DISK DRIVE

#### A. Hard disk drive model

The simulation used Maxtor HDD (Model 51536U3)[1].

Figure 3 shows the diagram of a single actuator arm seeking from any track to the target track.

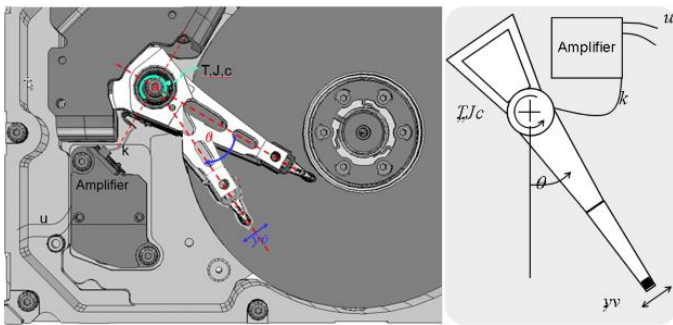


Figure 3: Diagram of a head move to another track.

The relationship between  $y = L\theta$  and  $T = k_1 u - k_2 \dot{\theta}$  that can get ODE equation =  $\frac{J}{L} \ddot{y} + \frac{(c+k_2)}{L} \dot{y} + \frac{k}{L} y = k_1 u$ . Thus the control design model is  $\dot{y} + 282.6\dot{y} + 3.9933 \times 10^6 y = 2.35 \times 10^8 u$ , where the term  $282.6\dot{y}$  is the viscous friction part of  $\tilde{T}_f$ , and the term  $3.9933 \times 10^6 y$  is a straight line estimate of  $\tilde{T}_c$ .

However, if consider the high-frequent resonance modes for more realistic model for the VCM actuator is shown in figure 4

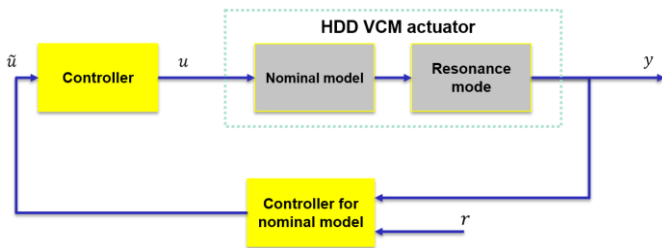


Figure 4: The control system for hard drive VCM

The nominal plan [1] is a tenth-order model for the actuator is obtained in equation (6.1) with the resonance mode is provided the equaltion (6.2) – (6.4).

$$G_v(s) = \frac{6.4013 \times 10^7}{s^2} \prod_{i=1}^4 G_{r,i}(s) \quad (6.1)$$

$$G_{r,1}(s) = \frac{0.912s^2 + 457.4s + 1.433 \times 10^8}{s^2 + 359.2s + 1.433 \times 10^8} \quad (6.2)$$

$$G_{r,2}(s) = \frac{0.7586s^2 + 962.2s + 2.491 \times 10^8}{s^2 + 789.1s + 2.491 \times 10^8} \quad (6.3)$$

$$G_{r,3}(s) = \frac{9.917 \times 10^8}{s^2 + 1575s + 9.917 \times 10^8} \quad (6.4)$$

$$G_{r,4}(s) = \frac{2.731 \times 10^8}{s^2 + 2613s + 2.731 \times 10^8} \quad (6.5)$$

The frequency response of the identified model is shown in figure 5.

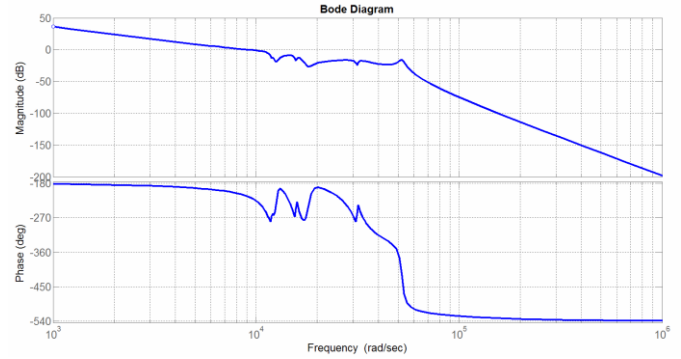


Figure 5: The frequency response of the plan with resonance mode.

#### B. Closed-Loop Application

Normally, if the controller does not add any under-damped poles to the closed-loop system, the natural frequency and damping ratio still follow those of the plant so that can get from figure 4. The simulation select natural frequency ( $\omega_n$ ) and damping ratio ( $\zeta_n$ ) from the poles are closely to zero poles:  $(1.21e^4, 0.015)$ ,  $(3.15e^4, 0.029)$ ,  $(1.58e^4, 0.03)$ ,  $(1.15e^4, 0.09)$ .

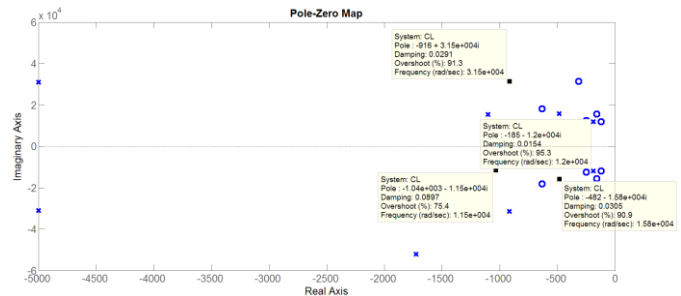


Figure 6 : Pole-Zero mapping.

The impulse sequence is developed by applied to the closed-loop system identifications using simple PID controller as an input shaper in Figure 7. The impulse sequence can be convolved with the reference position to create a shaped input that will cancel the residual vibrations.

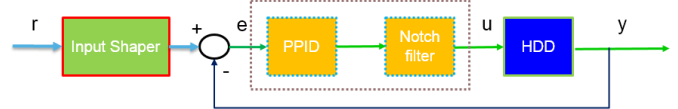


Figure 7 : Closed-loop-system block diagram with an input shaper.

For tracking, we need all impulse amplitudes to sum to one so that the shaped reference position will have the same end point as the original reference position. Therefore, in the three impulses case, the amplitudes and timing given in can be plotted as figure 8(a), where

$$K = e^{-\frac{\zeta\pi}{\sqrt{1-\zeta^2}}}$$

Figure 8(b) is shown the shaped step reference position, which is a result of convolving a step reference position  $r$  with the three-impulse sequence.

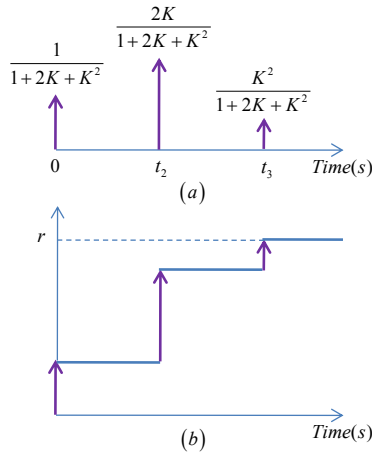


Figure 8 : (a) Three impulses. (b) Convolution of the impulse sequence with a step reference position [2].

This also shows that even though using more impulses provides more robustness, the shaped reference position will reach the end point slower at a later time  $t_N$ , where  $N$  is the number of impulses used.

#### IV. RESULTS AND CONCLUSION

The step response is shown in figure 9 after added input shaping is smoother than normal PPID, and the overshoot is lower than PPID. The simulation of time response is shown in table 1. The time response is related to the number of impulses. If adding more impulse, the test time will be increased. The simulation result suggests to add 1 impulse for minimizing the robustness, overshoot, and to add the time response is not much. The overall result can meet motivation targets.

Controller/ Time response	Delay time (ms)	Rise time (ms)	Peak time (ms)	Maximum overshoot (um)	Setting time (2%)	Steady-state error (t=0.25 ms)
PPID	0.000276	0.000717	0.001600	0.222000	0.003825	0.001000
PPID + Input Shaping 1 impulse	0.000540	0.000977	0.001720	0.203000	0.004050	0.001000
<b>PPID vs PPID + Input Shaping 1</b>	<b>0.000264</b>	<b>0.000260</b>	<b>0.000120</b>	<b>-0.019000</b>	<b>0.000225</b>	<b>0.000000</b>
PPID + Input Shaping 2 impulses	0.000730	0.001193	0.001957	0.198000	0.004250	0.001000
PPID + Input Shaping 3 impulses	0.000821	0.001289	0.002032	0.197000	0.004350	0.001000
PPID + Input Shaping 4 impulses	0.001039	0.001562	0.002313	0.191000	0.004600	0.001000

Table 1: The test time response.

The arbitrary reference position was convolved with a sequence of one impulse in real time producing a shaped input that cancels residual vibration of the system. The application of this technique is vast. It can be applied to dual actuator head or any systems suffering from vibrations during slewing. Nevertheless, the technique relies on the superposition principle of the linear system. No generalization over the nonlinear systems. Besides, the accuracy of the system's natural frequency and damping ratio is vital to the effectiveness of the technique.

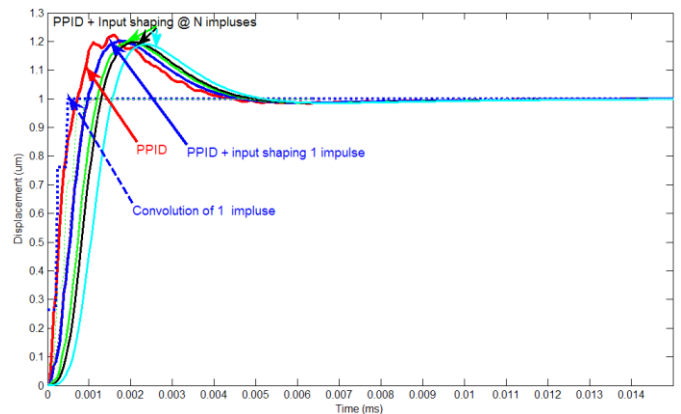


Figure 9 : Output response compare between normal PPID and Input shaping.

#### ACKNOWLEDGMENT

The author thanks the anonymous reviewers about comments and suggestions this work. This work is under HDD cluster scholarship of National Electronics and Computer Technology Center (NECTEC) Thailand and Seagate Technology (Thailand) Co.,Ltd. Also thanks to international college and college of data storage innovation (DSTAR), King Mongkut's institute of Technology Ladkrabang on cooperate this project study.

#### REFERENCES

- [1] Ben M. Chen, Tong H. Lee, Kemao Peng, and Venkatakrisnan, "Hard Disk Drive Servo Systems" 2<sup>nd</sup>, Springer-Verlag London Limited ,2006.
- [2] W. Chatlatanagulchai and K. Saeheng, "Real-time reference position shaping to reduce vibration in slewing of a very-flexible-joint robot," Journal of Research in Engineering and Technology, Vol. 6, No. 1, January 2009, pp. 51-66.
- [3] Chatlatanagulchai and C. Prutthapong, "Input shaping to reduce vibration in human-operated very-flexible-link robot manipulator," KKU Engineering Journal, Vol. 36, No. 1, January 2009.
- [4] Li Yi, M. Tomizuka, "Two Degree-of-Freedom control with adaptive robust control for hard disk servo systems", IEEE/ASME Trans. Mechatron., 4(1), 1999 17-24.